RESEARCH ARTICLE

WILEY

Down syndrome is accompanied by significantly reduced cortical grey–white matter tissue contrast

Anke Bletsch[1] | Caroline Mann[1] | Derek S. Andrews[2] | Eileen Daly[2] | Giles M. Y. Tan[2] | Declan G. M. Murphy[2] | Christine Ecker[1,2]

[1]Department of Child and Adolescent Psychiatry, Psychosomatics and Psychotherapy, University Hospital Frankfurt am Main, Goethe-University Frankfurt am Main, Frankfurt am Main, Germany

[2]Department of Forensic and Neurodevelopmental Sciences, and the Sackler Institute for Translational Neurodevelopmental Sciences, Institute of Psychiatry, Psychology and Neuroscience, King's College, London, United Kingdom

Correspondence
Anke Bletsch, Department of Child and Adolescent Psychiatry, Goethe-University Frankfurt, Deutschordenstrasse 50, 60528 Frankfurt am Main, Germany.
Email: Anke.Bletsch@kgu.de

Abstract

Increased cortical thickness (CT) has been reported in Down syndrome (DS) during childhood and adolescence, but it remains unclear, which components of the neural architecture underpin these increases and if CT remains altered in adults. Among other factors, differences in CT measures could be driven by reduced tissue contrast between grey and white matter (GWC), which has been reported in neurodegenerative disorders, such as Alzheimer's disease. Using structural magnetic resonance imaging, we therefore examined differences in CT and GWC in 26 adults with DS, and 23 controls, to (1) examine between-group differences in CT in adulthood, (2) establish whether DS is associated with significant reductions in GWC, and (3) determine the influence of GWC variability on between-group differences in CT. As hypothesized, we observed that DS was accompanied by wide-spread increases in CT, and significantly reduced GWC in several large clusters distributed across the cortex. Out of all vertices with a significant between-group difference in CT, 38.50% also displayed a significant reduction in GWC. This percentage of overlap was also statistically significant and extremely unlikely to be obtained by chance ($p = .0002$). Differences in GWC thus seem to explain some, although not all, of the differences in CT observed in DS. In addition, our study is the first to extend previous *in vivo* reports of altered CT in DS during childhood and adolescence to older adults, implying that the regional pattern of neuroanatomical differences associated with DS remains stable across the lifespan.

KEYWORDS
adulthood, brain anatomy, cortical thickness

1 | INTRODUCTION

Down syndrome (DS) is a genetic condition caused by a trisomy of chromosome 21. In addition to distinctive physical features (Weijerman & de Winter, 2010), DS is associated with intellectual disability and various medical conditions such as cardiovascular and immunological abnormalities (for a review, see Abanto et al., 2011). Moreover, DS is accompanied by an atypical development of the brain, with (a) significantly reduced brain size overall (Haier et al., 1995), (b) developmental perturbations to the configuration of the underlying cortical microstructure (e.g., aberrant dendritic development and atypical neocortical lamination; Becker, Mito, Takashima, & Onodera, 1991; Golden & Hyman, 1994; Mrak & Griffin, 2004), and (c) significant reductions in overall neuronal numbers (Guidi, Ciani, Bonasoni, Santini, & Bartesaghi, 2011). Many of these structural alterations have been linked to ongoing neurodegeneration (Wisniewski, Wisniewski, & Wen, 1985). The specific neurobiological mechanisms that underpin the cortical malformation of the brain in DS, however, remain poorly understood.

To date, there are few neuroimaging studies examining atypical brain anatomy in DS *in vivo*. Structural magnetic resonance imaging

(MRI) studies typically report significantly reduced total brain volume in DS, with commensurate reductions in total grey and white matter volume (Kates, Folley, Lanham, Capone, & Kaufmann, 2002; Pearlson et al., 1998; Pinter, Eliez, Schmitt, Capone, & Reiss, 2001). Such volumetric reductions are particularly prominent in the frontal and occipital lobes, with relative preservation of the parietal cortices (Pinter et al., 2001). It therefore seems that not all brain regions are equally affected in DS, but that there is region-dependent variability in the degree of cortical abnormality observed. Thus, volumetric differences in the brain of individuals with DS might be driven by distinct underlying mechanisms affecting brain volume in a region-specific manner.

To date, however, only one neuroimaging study has linked the differences in brain volume to different underlying mechanisms in DS in children, adolescents and young adults. In this study, Lee et al. (2016) investigated volumetric differences in DS based on its two constituent components (i.e., cortical thickness (CT) and surface area), which are known to represent different developmental trajectories and aspects of the cortical architecture (Geschwind & Rakic, 2013). It was reported that decreased cortical volume in DS was predominately driven by significant reductions in surface area, particularly in frontal and temporal regions (Lee et al., 2016). Measures of CT, on the other hand, were significantly increased in DS. CT measures have previously been linked to neuronal numbers (Geschwind & Rakic, 2013; Rakic, 1988) which—in turn—have been consistently reported to be decreased in the cortex of DS individuals (Chakrabarti, Galdzicki, & Haydar, 2007; Guidi et al., 2008; Guidi et al., 2011). It therefore remains unclear, which components of the neural architecture underpin increased CT in DS and if CT alterations remain stable across the human lifespan.

One neuroanatomical feature that could affect *in vivo* measures of CT in DS is grey–white matter tissue contrast (GWC). By definition, MRI-based measures of CT are computed as the closest distance from the grey–white matter boundary to the grey matter-cerebrospinal fluid (CSF) boundary at each location (i.e., vertex) on the cortical surface (Fischl & Dale, 2000). *In vivo* measures of CT therefore heavily rely on the ability to clearly delineate the grey–white matter boundary, which is—in turn—dependent on tissue contrast. In neurodegenerative conditions, such as Alzheimer's Disease (AD), the GWC has been shown to be significantly decreased relative to typically developing (TD) controls (Grydeland, Westlye, Walhovd, & Fjell, 2013; Jefferson et al., 2015; Salat et al., 2011), and also reduces in healthy aging (Salat et al., 2009; Westlye et al., 2009), potentially driven by reduced tissue integrity and myelination within the white matter (Davatzikos & Resnick, 2002; Salat et al., 2009; Vidal-Piñeiro et al., 2016). As DS has been linked with both neurodegeneration and white matter atypicalities (Holtzman et al., 1996; Lott & Head, 2001; Olmos-Serrano et al., 2016; Wisniewski & Schmidt-Sidor, 1989), it is likely that the GWC is also altered in DS. The objectives of this study were therefore threefold: (a) to examine between-group differences in CT in adult individuals with DS relative to controls, (b) to establish whether DS is associated with significant reductions in GWC of the brain, and (c) to determine the influence of GWC variability on between-group differences in CT.

2 | MATERIALS AND METHODS

2.1 | Participants

Overall, 26 adults with DS (20 males and 6 females) and 23 TD controls (17 males and 6 females) aged 18–51 years were included in this study. Adults with DS were recruited across England and Scotland. The study was conducted at the South London and Maudsley NHS Foundation Trust in London. We included men and women with DS aged 18 years or older without a co-morbid diagnosis of dementia. Karotyping was used to confirm a diagnosis of DS in all participants. Dementia status was assessed using the International Statistical Classification of Disease version 10 (ICD-10) criteria (WHO, 1992). Groups did not significantly differ in age or sex (Supporting Information, Table 1). Of the 26 DS participants, 9 individuals had a prior history of psychiatric disorder(s) including depression, anxiety, autism spectrum disorder (ASD), and attention-deficit hyperactivity disorder (ADHD). 7 DS individuals were taking psychotropic medication at the time of study (e.g., antidepressants, neuroleptics, and hypnotics). None of the TD controls had a history of psychiatric disorders. The project was approved by the national research ethics service (NRES), and written informed consent was obtained from participants and their carers. If this was not possible, proxy consent was obtained from their legal representatives. All participants also satisfied MRI safety requirements, and spoke English as their native language.

2.2 | Cognitive assessment

Cognitive abilities in the DS group were assessed using the Cambridge Cognitive Examination (CAMCOG) and the British Picture Vocabulary Scale (BPVS). The CAMCOG (Huppert, Brayne, Gill, Paykel, & Beardsall, 1995) has been validated for use with adults with DS (Hon, Huppert, Holland, & Watson, 1999), and provides a measure of general cognitive function, including measures of episodic memory, orientation, language, attention, praxis, and executive function. It is therefore appropriate for assessing cognitive functioning in individuals with intellectual disability. The BPVS (Dunn, Dunn, Whetton, & Burley, 1997) was used to assess receptive vocabulary, which is highly correlated with full-scale IQ, to give an additional indication of overall cognitive function. In the TD group, the Wechsler Abbreviated Scale of Intelligence (WASI) was used to assess general cognitive functioning. For each participant, neuropsychological testing was completed within 6 months of scanning (for group means, see Supporting Information, Table 1).

2.3 | MRI data acquisition

All participants were scanned at the Maudsley Hospital, Institute of Psychiatry, Psychology and Neuroscience, London, UK, using a 1.5-T GE Signa System (General-Electric, Milwaukee, WI). High-resolution structural T1-weighted volumetric images were acquired with full head coverage, 160 contiguous slices (1.2-mm thickness, with 1.2 × 1.2-mm in-plane resolution), a 256 × 256 × 160 matrix and a repetition time/echo time (TR/TE/TI) of 11/2.8/300 ms (flip angle = 18 in., FOV = 31 cm). A (birdcage) 8-channel head coil was used for

radiofrequency transmission and reception. Consistent image quality was ensured by a semi-automated quality control procedure.

2.4 | Cortical reconstruction using FreeSurfer

All individual T1-weighted scans were initially screened by a radiologist to exclude images with visible clinical abnormalities or large-scale movement artifacts. Scans of insufficient quality (e.g., apparent movement, clinical abnormalities) were excluded from the analysis a priori. Within the DS group, we started off with 27 scans. Here, one scan was excluded due to the existence of severe motion artifacts (dropout 4%). We did not exclude any participants in the control group. For the 26 participants in the DS group, at least one (sometimes two) structural scans were available. Here, we usually utilized the first scan. FreeSurfer v5.3.0 software (http://surfer.nmr.mgh.harvard.edu/) was used to derive models of the cortical surface for each T1-weighted image. These well-validated and fully automated procedures have been extensively described elsewhere (Dale, Fischl, & Sereno, 1999; Fischl, Sereno, & Dale, 1999; Fischl & Dale, 2000; Jovicich et al., 2006; Ségonne et al., 2004). In brief, a single filled white-matter volume was generated for each hemisphere after intensity normalization, extracerebral tissue was cropped, and image segmentation performed using a connected components algorithm. A triangular tessellated surface was then generated for each white-matter volume by fitting a deformable template, resulting in a cortical mesh for the pial (i.e., outer) and white-matter (i.e., inner) surface. The resulting surface models were visually inspected for reconstruction errors, and surface reconstructions with visible inaccuracies were further excluded from the statistical analysis. In one individual with DS, the FreeSurfer reconstruction had severe topological defects when analyzing the first scan. For this participant, we utilized the second scan.

Measures of CT were computed as the closest distance from the grey–white matter boundary to the grey matter–cerebrospinal fluid boundary at each vertex on the tessellated surface (Fischl et al., 1999). We also computed mean CT across hemispheres for each participant. To improve the ability to detect population changes, each parameter was smoothed using a 15-mm gaussian surface-based smoothing kernel.

2.5 | Grey-to-white matter ratio and grey and white matter tissue intensity measures

Grey matter tissue intensities (GMI) were sampled continuously across different cortical layers starting from the grey-white matter boundary (i.e., the white matter surface) up to 50% into the thickness of the cortical ribbon where the outer pial surface equaled 100% (Supporting Information, Figure 1). Sampling points were separated by projection fraction intervals of 10%, thus yielding a set of five GMI measures (at 10%, 20%, 30%, 40%, and 50%). The outer 50% of the cortical sheet was not sampled to assure that sampling was performed entirely within the grey matter and not confounded by voxels composed of CSF. White matter tissue intensity (WMI) was measured at 1.0 mm into the white matter from the white matter surface (Supporting Information, Figure 1).

The GWC at projection fraction (i) was then calculated as the percentage of GMI to WMI at each cerebral vertex (j) (Salat et al., 2009):

$$GWC_{i,j} = 100 \times (WMI_{1.0mm,j} - GMI_{i,j}) / 0.5 \times (WMI_{1.0mm,j} + GMI_{i,j}).$$

By definition, a decrease in GWC reflects decreases in contrast between the grey matter tissue intensity measured at projection fraction j and the white matter tissue intensity measured at 1.0 mm into the white matter. We also examined the tissue contrast when GMI was sampled at the grey–white matter boundary (i.e., at 0% projection fraction).

To determine the influence of grey and white matter intensity on the GWC, we also extracted the absolute grey (GMI) and white matter intensities (WMI) at each cerebral vertex following nonuniform (NU) intensity correction and normalization (i.e., scaling of mean intensity of the white matter to 110) of the images in FreeSurfer at a projection fraction of 30% CT, and at 1.0 mm into the white matter (FreeSurfer default for the computation of the GWC). All surface overlays were smoothed using a 15-mm full-width at half-maximum (FWHM) Gaussian kernel prior to statistical analyses.

2.6 | Statistical analyses

Statistical analysis was conducted using the SurfStat toolbox (http://www.math.mcgill.ca/keith/surfstat/) for Matlab (R2016a; MathWorks). Vertex-wise statistical analyses of CT, GWC, and GMI/WMI (Y) were estimated by regression of a general linear model (GLM) at each vertex i, with (a) diagnostic group and biological gender as categorical fixed-effect factors and (b) age as continuous covariate:

$$Y_i = \beta_0 + \beta_1 Group + \beta_2 Gender + \beta_3 Age + \varepsilon_i,$$

where ε_i is the residual error at vertex i.

For the investigation of between-group differences in CT, mean CT computed across the cortex was included as a covariate. All between-group differences were estimated from the corresponding coefficient β_1, normalized by the corresponding standard error, respectively. Corrections for multiple comparisons across the whole brain were performed using "random field theory" (RFT)-based cluster analysis for nonisotropic images using a cluster-based significance threshold of $p < .05$ (two-tailed) (Worsley, Andermann, Koulis, MacDonald, & Evans, 1999).

To compare frequencies of unique or overlapping differences in each morphometric parameter, the resulting spatially distributed patterns of differences unique to CT and/or GWC, as well as their overlap were then compared using a χ^2 test (i.e., contingency table), testing the null hypothesis that differences in CT and GWC are equally distributed. Furthermore, a simulation strategy was used to assess whether the observed degree of overlap between differences in CT and GWC is consistent with the idea of two spatially (in)dependent patterns. This hypothesis was tested on the basis of $N = 5000$ randomly generated difference maps (i.e., maps containing random t values, thresholded at $p < .05$) for CT and GWC. The extent of overlap (i.e., number of

vertices with differences in CT and GWC) was then assessed in each of the 5,000 overlapping patterns to derive a probability value of obtaining a given percentage of overlap on the basis of randomly varying patterns of differences. As we were interested in determining the influence of GWC variability on between-group differences in CT, we used CT as a mask and only looked for variability in GWC in all vertices with a significant between-group difference in CT.

3 | RESULTS

3.1 | Participant demographics and global brain measures

There were no significant differences in the distributions of age or sex between DS and TD controls (Supporting Information, Table 1). In line with previous research, individuals with DS had significantly reduced total brain volume ($t(47) = -8.62$, $p < .0001$), total grey matter volume ($t(47) = -8.55$, $p < .0001$), and total white matter volume ($t(47) = -7.79$, $p < .0001$).

3.2 | Between-group difference in CT

Following correction for multiple comparisons (RFT-based cluster corrected, $p < .05$, two-tailed), individuals with DS had significantly increased CT compared to TD controls in several large and spatially distributed clusters across the cortex. The CT increases were observed in extended areas of the bilateral frontal lobes including (a) the dorsolateral and ventrolateral prefrontal cortices (approximate Brodmann Area [BA] 8), (b) the medial prefrontal cortex (BA10), and (c) the orbitofrontal cortex (BA47). Furthermore, we found significantly increased CT in DS in several areas of the occipital and parietal lobes (bilateral) including (d) the lateral and medial occipital cortex (BA18) and (e) the medial and superior parietal cortices (BA7) (see Figure 1a and Table 1 for details). Relative to TD controls, individuals with DS had significantly reduced CT in the bilateral anterior temporal lobes (BA13) and in the right precentral gyrus (BA6) (see Figure 1a and Table 1 for details).

3.3 | Between-group difference in GWC

Across the different projection fractions (i.e., 0, 10, 20, 30, 40, and 50% CT), we found that GWC was significantly reduced in individuals with DS compared to TD controls in several clusters across the cortex. These reductions were observed in extended areas of the frontal and temporal lobes in both hemispheres centering on the superior temporal gyrus (BA34) and the inferior frontal gyrus (BA44). The GWC was also reduced in the right lateral occipital cortex (BA18) and the bilateral subgenual cingulate (BA25) in DS individuals relative to TD controls (see Figure 1b and Table 2 for details). In these regions, DS individuals thus had a significantly reduced tissue contrast between grey and white matter. The reductions in GWC were most extensive closest to the grey–white matter boundary, and decreased in spatial extent with increasing projection fraction into the cortex (i.e., away from the grey–white matter boundary). There were no clusters where participants

with DS showed a significant increase in GWC as compared to TD controls.

3.4 | Spatial overlap of between-group differences in CT and GWC

When examining the spatial overlap between the patterns of between-group differences in CT and GWC, we found that across hemispheres, the number of vertices with a between-group difference in CT ($n = 160,674$) significantly exceeded the number of vertices with atypical GWC ($n = 100,421$) in DS (χ^2 ($df = 1$) $= 13,905$, $p < .001$). More specifically, out of all vertices with a significant between-group difference in CT, 61,867 vertices (i.e., 38.50%) also displayed a significant reduction in GWC (Figure 2). Similar proportions were also observed, when examining clusters with significant in-/or decreased CT separately, where 39.52% of differences in GWC "explained" (i.e., overlapped with) significantly increased CT, and 34.45% of GWC vertices overlapped with vertices displaying a significant decrease in CT. Simulations revealed that the probability of obtaining the same degree of overlap (i.e., 38.50%) or higher by chance is less than $p = .0002$.

3.5 | Between-group difference in absolute grey and white matter intensities

To identify whether the observed differences in GWC were driven by intensity differences in grey or white matter—or a combination of both —we subsequently examined between-group differences in absolute grey and white matter intensities at a projection fraction of 30% and -1.0 mm, respectively (i.e., FreeSurfer defaults). Compared to TD controls, individuals with DS had significantly reduced GMI and WMI in several large clusters distributed across the cortex. For both tissue types, these reductions were observed predominantly in the temporal and cingulate cortices of both hemispheres, and in the left parietal lobe and the right frontal lobe, centering on the right fusiform gyrus (BA36), the left occipitotemporal region (BA37), the bilateral subgenual cingulate cortex (BA25), the left postcentral gyrus (BA3), and the right superior frontal gyrus (BA8), respectively (see Figure 3 and Supporting Information, Table 2 for details). There were no brain regions where individuals with DS had significantly increased GMI or WMI relative to TD controls. Thus, it seems that the differences in tissue contrast between grey and white matter in DS cannot easily be attributed to variability in one tissue type, but are driven by significant reductions in both, grey and white matter, as well as by their proportional difference (i.e., a proportionally larger reduction in one tissue type relative to the other).

4 | DISCUSSION

This study examined whether DS is associated with significant alterations in CT during adulthood and reductions in GWC compared to TD controls, and whether variability in GWC might explain the between-group differences in CT. We observed that overall, measures of CT were significantly increased in DS, particularly in frontal, parietal and
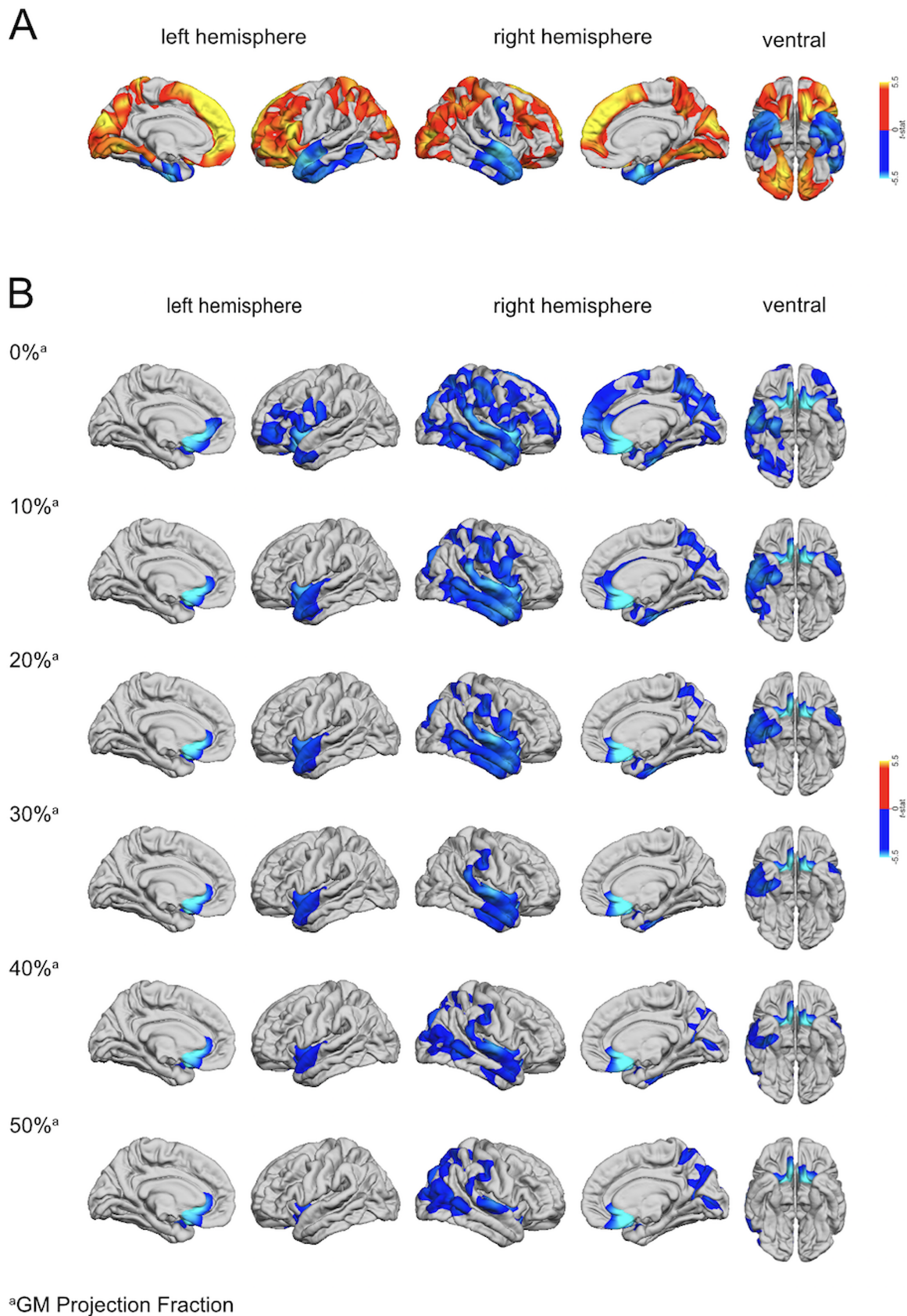
FIGURE 1 (a) Regions of increased and decreased cortical thickness (CT) in DS compared to TD controls. The blue to cyan colorscale indicates brain regions with significantly decreased CT in DS relative to TD controls (RFT-based cluster corrected $p < .05$, two-tailed). The orange to yellow colorscale indicates brain regions with significantly increased CT in DS compared to TD controls. (b) Regions with significantly decreased grey–white matter tissue contrast (GWC) in DS (blue colorscale) compared to TD controls (RFT-based cluster corrected $p < .05$, two-tailed) at the grey–white matter boundary (i.e., 0%), and at different CT projection fractions (i.e., sampled from 0% to 50% into the thickness of the cortical ribbon from the pial surface for grey matter in steps of 10%)
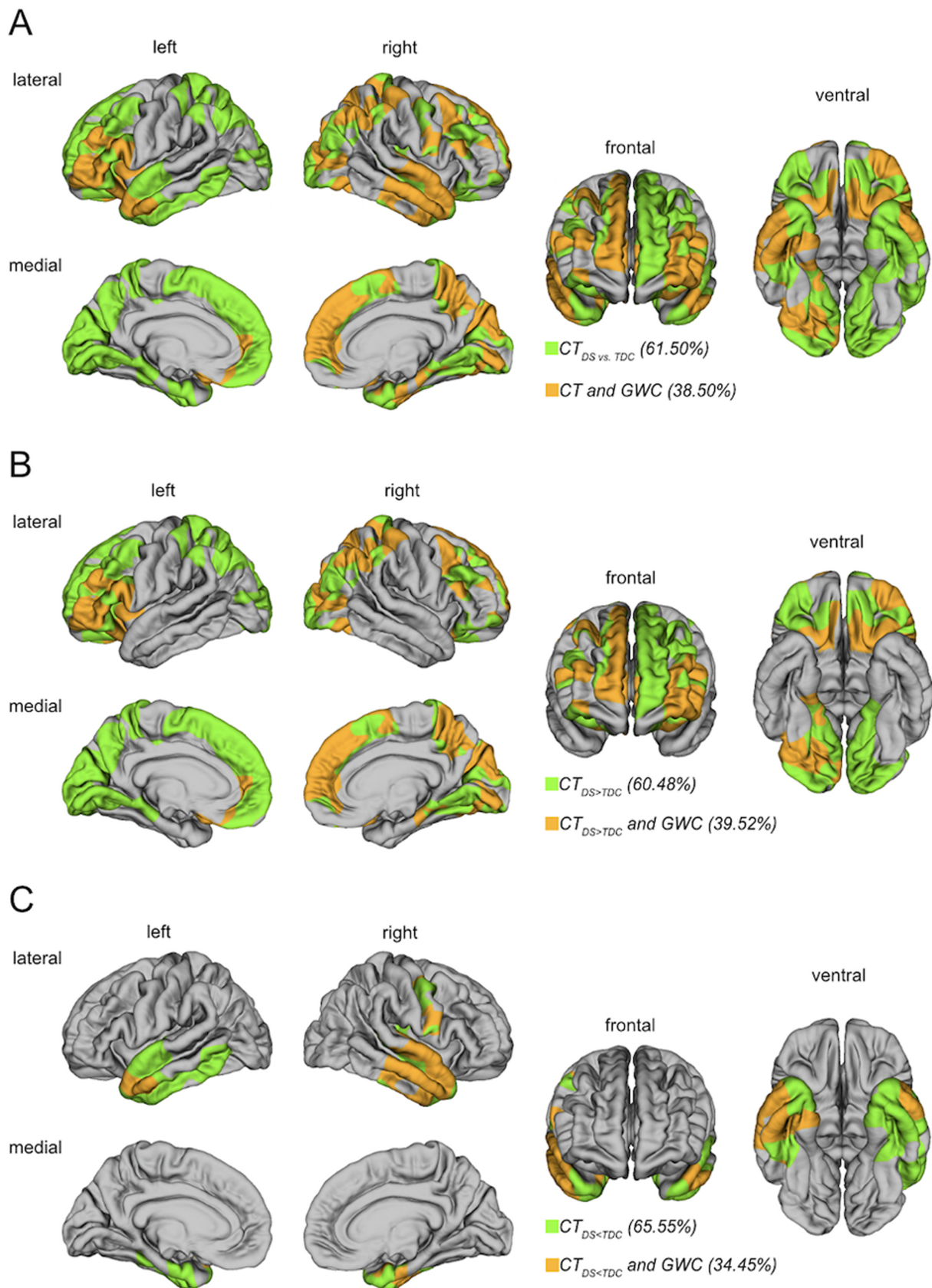
FIGURE 2 Spatial overlap between the patterns of between-group differences in GWC and CT. In all overlap maps, the clusters of significant CT differences were applied as a mask (i.e., CT differences that may be explained by GWC differences). (a) Spatial overlap between CT and GWC clusters regardless of sign (i.e., positive or negative differences in CT). (b) Spatial overlap between regions with significantly increased CT in DS relative to TD controls (TDC) ($CT_{DS} > CT_{TDC}$) and differences in GWC. (c) Spatial overlap between regions with significant decreases in CT in DS relative to TD controls (TDC) ($CT_{DS} < CT_{TDC}$) and differences in GWC
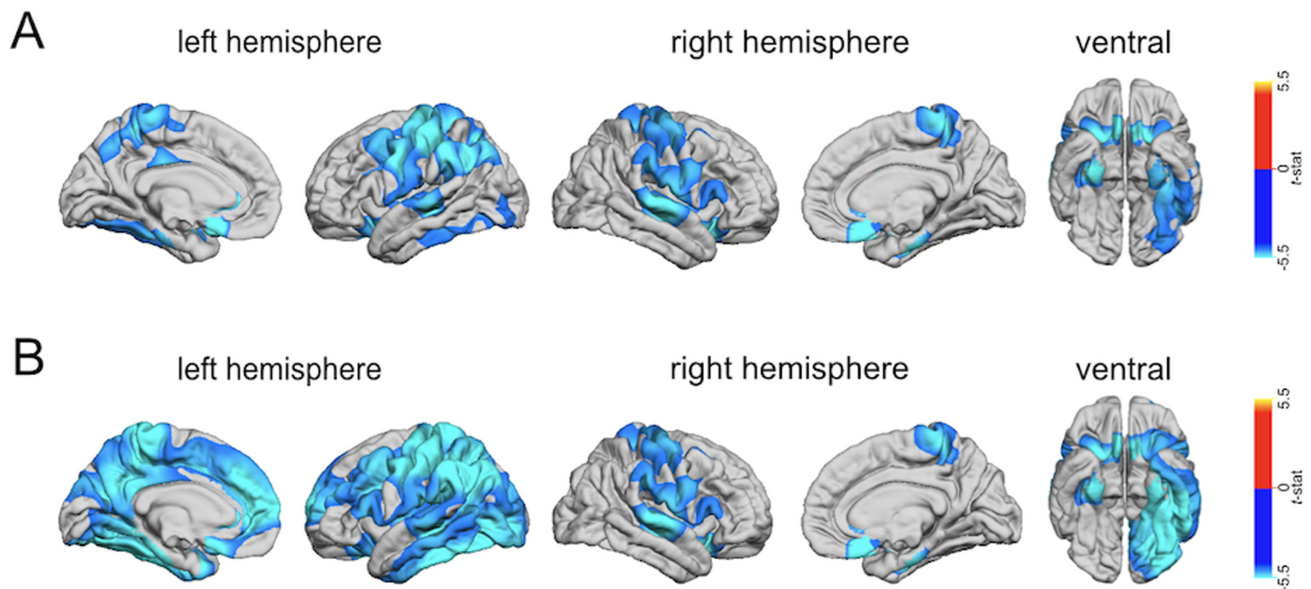
FIGURE 3 Clusters with significantly decreased grey (GMI) or white (WMI) matter tissue intensity in DS compared to TD controls (RFT-based cluster corrected, $p < .001$, two-tailed), sampled at (a) 1.0 mm into the white matter starting from the grey–white matter boundary for WMI (upper panel), and measured at (b) 30% into the thickness of the cortical ribbon from the pial surface for GMI (lower panel)

occipital regions, while the GWC was reduced in DS relative to controls. Out of all vertices with a significant between-group difference in CT, 38.50% also displayed a significant reduction in GWC. The probability of obtaining the same degree of overlap or higher by chance is less than $p = .0002$, indicating that the two measures are spatially dependent. It is thus likely that some of the differences in CT in DS are driven by differences in GWC, even though reduced GWC cannot explain all differences in CT. Taken together, our findings suggest that the tissue contrast between grey and white matter is less well-defined in DS, and the characteristic pattern of CT differences—with decreases in temporal regions and increases in other regions of the cortex—remains stable across the human lifespan in DS.

In this study, we first examined differences in CT between individuals with DS and TD controls. To date, alterations in CT in DS relative to controls have only been studied in one *in vivo* study examining individuals during childhood and young adulthood (Lee et al., 2016). Here, we therefore extended the analysis of between-group differences in CT in DS by examining older adults. We established that CT is significantly increased in DS during adulthood, particularly in frontal, parietal, and occipital regions. Significant decreases were observed in temporal regions and one small cluster in the right frontal cortex. Overall, our findings are therefore in accordance with the earlier neuroimaging study by Lee et al. (2016) in children, adolescents, and young adults, who reported significantly increased CT in similar brain regions as reported here and decreased CT in two small regions of the temporal lobes. Moreover, our study builds upon this previous report by suggesting that (a) differences in CT are not only present in DS from childhood to young adulthood (5–24 years of age) (Lee et al., 2016), but also older adults with the condition (i.e., from 18 to 51 years), and that (b) the patterns of CT differences in DS seem to remain stable across the human life span in terms of their regional composition.

Second, we tested the hypothesis that DS is accompanied by significantly reduced tissue contrast relative to TD controls, which may affect the reliability of *in vivo* estimates of CT. As expected, we found that the GWC in DS was significantly reduced across the cortex, particularly in the temporal, frontal, and occipital lobes. This is of importance as reduced GWC has previously been suggested to be a marker of neurodegeneration (Grydeland et al., 2013; Salat et al., 2011; Westlye et al., 2009), and is also characteristic of the "aging process" in the TD brain (Salat et al., 2009; Westlye et al., 2009). Here, the typical age-related decrease in GWC has primarily been linked to declining tissue integrity within the cortical white matter (Davatzikos & Resnick, 2002; Salat et al., 2009), and the degree of myelination in the superficial white matter under the cortical mantle (Salat et al., 2009; Vidal-Piñeiro et al., 2016; Westlye et al., 2009). In DS, white matter atypicalities—such as delayed myelination (Ábrahám et al., 2012; Becker et al., 1991; Dambska & Laure-Kamionowska, 1990; Wisniewski & Schmidt-Sidor, 1989) and progressive early demyelination (Haydar & Reeves, 2012)—have previously been reported in several cortical regions.

To establish whether the observed differences in GWC in our sample were driven by intensity differences in grey or white matter, or a combination of both, we also examined between-group differences in absolute grey and white matter tissue intensities in the present study. We found that the intensities of both tissue types were significantly reduced in DS individuals relative to TD controls. However, while the affected brain regions constituted several large and spatially distributed clusters across the cortex, we found little overlap between the patterns of differences in absolute signal intensities and GWC. Thus, it seems that differences in tissue contrast between grey and white matter in DS cannot easily be attributed to variability in one tissue type, but are driven by significant reductions in both grey and white matter, as well as their proportions (i.e., a proportionally larger reduction in either grey or white matter relative to the other).

TABLE 1 Clusters with significantly increased and decreased cortical thickness (CT) in DS relative to TD controls (TDC)

Contrast	Cluster	Region labels	Side	BA (t_{max})	Vertices	Talairach x	Y	z	t_{max}	$p_{cluster}$
DS > TDC	1	Superior parietal cortex, inferior parietal cortex, precuneus cortex	R	18	40,501	8	−84	20	6.55	6.46×10^{-6}
	2	Superior parietal cortex, precuneus cortex, lateral occipital cortex	L	7	35,816	−25	−47	58	7.10	6.46×10^{-6}
	3	Superior frontal gyrus, rostral middle frontal gyrus, lateral orbital frontal cortex	L	8	31,480	−8	33	43	9.44	6.46×10^{-6}
	4	Superior frontal gyrus, rostral middle frontal gyrus, caudal middle frontal gyrus	R	10	16,238	9	54	13	7.59	6.50×10^{-6}
	5	Lateral orbital frontal cortex, pars orbitalis, medial orbital frontal cortex	R	47	4,354	15	21	−14	7.56	9.09×10^{-3}
DS < TDC	1	Superior temporal gyrus, middle temporal gyrus, inferior temporal gyrus	R	13	15,141	40	−22	−3	−7.46	8.83×10^{-6}
	2	Inferior temporal gyrus, superior temporal gyrus, fusiform gyrus	L	13	14,165	−39	−19	−6	−6.21	1.28×10^{-5}
	3	Precentral gyrus	R	6	2,979	39	−9	39	−5.08	4.65×10^{-2}

Note. Region labels listed include up to three regions with the highest *t* values; side = hemisphere; L = left; R = right; BA = approximate Brodmann area at t_{max}; vertices = number of vertices within the cluster; t_{max} = maximum *t*-statistic within the cluster; $p_{cluster}$ = cluster-corrected *p* value.

We further investigated whether reductions in GWC could explain the between-group differences in CT by examining the spatial overlap between the difference patterns for CT and GWC. We found that out of all vertices with a significant between-group difference in CT, 38.50% also displayed a significant reduction in GWC. Simulations revealed that the probability of obtaining the same degree of overlap

TABLE 2 Clusters with significant reductions in grey–white matter tissue contrast (GWC) in DS relative to TD controls

Cluster	Region labels	Side	Projection fraction	BA (t_{max})	Vertices	Talairach x	y	z	t_{max}	$p_{cluster}$
1	Superior parietal cortex, precuneus cortex, superior frontal gyrus	R	0	34	81,115	15	7	−14	−10.58	3.68×10^{-6}
2	Superior parietal cortex, superior temporal gyrus, middle temporal gyrus	R	10	34	58,818	15	7	−14	−9.99	2.93×10^{-6}
3	Superior parietal cortex, precuneus cortex, postcentral gyrus	R	20	44	18,739	57	6	21	−3.71	4.15×10^{-5}
4	Superior parietal cortex, inferior parietal cortex, precuneus cortex	R	50	18	25,321	25	−75	19	−3.60	1.60×10^{-5}
5	Superior temporal gyrus, middle temporal gyrus, inferior temporal gyrus	R	20	25	23,968	6	13	−9	−9.73	4.55×10^{-6}
6	Superior temporal gyrus, supramarginal gyrus, middle temporal gyrus	R	30	34	20,138	14	7	−14	−9.56	9.80×10^{-6}
7	Superior temporal gyrus, superior parietal cortex, inferior parietal cortex	R	40	34	33,620	14	7	−13	−9.58	2.68×10^{-6}
8	Superior temporal gyrus, medial orbital frontal cortex, insula	R	50	25	8,438	13	8	−13	−9.36	4.97×10^{-3}
9	Rostral middle frontal gyrus, pars opercularis, precentral gyrus	L	0	44	10,599	−51	5	7	−3.55	1.81×10^{-3}
10	Insula, lateral orbital frontal cortex, medial orbital frontal cortex	L	0	34	8,707	−14	5	−13	−10.57	2.00×10^{-3}
11	Superior temporal gyrus, insula, lateral orbital frontal cortex	L	**10**, 20, 30, 40, 50	34	8,971	−14	5	−13	−9.48	3.09×10^{-3}

Note. Region labels include up to three regions with the highest *t* values; side = hemisphere; L = left; R = right; projection fraction = CT projection fraction. In clusters referring to more than one projection fraction, the projection fraction in bold is the one with the smallest *p* value. The other values listed (i.e., BA(t_{max}), vertices, Talairach coordinates, t_{max}, and p_{max}) also refer to the projection fraction with the smallest *p* value. BA = approximate Brodmann area at t_{max}; vertices = number of vertices within the cluster; t_{max} = maximum *t* statistic within the cluster; $p_{cluster}$ = cluster-corrected *p* value.

or higher by chance is less than $p = .0002$. There was thus a significant overlap between the patterns of between-group differences in CT and GWC, which was unlikely due to random variability in both features. Our finding is hence consistent with the hypothesis that differences in CT and GWC are at least partly spatially dependent. This means that some of the differences in CT in DS may be driven by differences in GWC, even though reduced GWC cannot explain all differences in CT. For example, 61.50% of CT differences in our study were not being accounted for by variability in GWC, and are therefore likely to be caused by alternative mechanisms. For example, many regions where we observed a significant increase in CT in DS (i.e., frontal and occipital regions) undergo a period of apoptosis and extensive synaptic pruning during childhood and adolescence (Huttenlocher, 1984, 1990; Huttenlocher & Dabholkar, 1997), which leads to a thinning of the cortical mantle during brain maturation (Gogtay et al., 2004; Raznahan et al., 2011; Shaw et al., 2008; Vandekar et al., 2015; Wierenga, Langen, Oranje, & Durston, 2014). On the other hand, many of the brain regions where we observed significantly reduced CT in DS individuals (e.g., temporal lobes), are typically characterized by cortical thickening in early adolescence (Vandekar et al., 2015), potentially due to a second occurrence of synaptogenesis or increases in neuropil (Giedd et al., 1999). It thus seems that in addition to myelination-dependent effects, the neural mechanisms that underpin brain maturation in the TD brain may be perturbed in DS. Among others, these mechanisms also include impaired neurogenesis, as reported above (Benavides-Piccione et al., 2004; Chakrabarti et al., 2007; Guidi et al., 2008; Guidi et al., 2011; Schmidt-Sidor, Wisniewski, Shepard, & Sersen, 1990; Sylvester, 1983), and increased apoptosis (Guidi et al., 2008; Haydar, Nowakowski, Yarowsky, & Krueger, 2000; Rueda, Flórez, & Martínez-Cué, 2013). It will therefore be essential in the future to conduct a more detailed age-related histological investigation of the grey–white matter boundary in DS, in addition to the cortical grey matter neuroarchitecture, to elucidate the cortial mechanism underpinning our *in vivo* differences in CT and GWC.

Our study has a number of limitations. First, brain anatomy in DS was compared to the neuroanatomy of TD individuals, rather than a group of individuals with a learning disability. Thus, we cannot rule out the possibility that our findings also reflect differences in intellectual abilities, in addition to differences caused by genetic variability in chromosome 21. However, as intellectual impairment is an inherent feature of DS, covarying for cognitive abilities would mostly "partial out" statistical effects of interest. Moreover, it has been shown that different groups of individuals with intellectual disability, such as idiopathic intellectual disability or Fragile X syndrome, show distinct patterns for CT variability (Meguid et al., 2012; Zhang et al., 2011).

Second, it is possible that some of our results are confounded by head motion, which has previously been shown to reduce tissue contrast, and also affects measures of CT. Head motion is of particular importance in DS individuals, which are difficult to scan due to their intellectual disability, and would be expected to move more than neurotypical controls (Backhausen et al., 2016). However, increased motion is generally associated with a significant reduction of CT (Pardoe, Kucharsky Hiess, & Kuzniecky, 2016; Reuter et al., 2015), particularly in precentral and dorsolateral prefrontal regions, where we

either observed no differences in DS, or a significant increase in our sample. Moreover, even though motion artifacts have also been shown to reduce the tissue contrast in general, these reductions are typically bilateral (Pardoe et al., 2016). In our study, however, the reductions we observed in GWC were mostly found in the right hemisphere. Last, we observed that there was only an 38.50% overlap between differences in CT and GWC. This means, that the remaining 61.50% of CT differences remain "unexplained" by significant reductions in tissue contrast potentially caused by motion. The characteristic pattern of between-group differences in CT—with decreases in DS in temporal regions and increases in frontal, occipital, and parietal regions—is therefore unlikely to be caused by motion alone. However, differences in CT and GWC should be interpreted with care, and a more thorough investigation of the impact of motion artifacts on between-group differences in surface anatomy in DS is required in the future.

Third, within the scope of this study, we did not examine brain–behavioural associations (e.g., correlations between measures of symptom severity and brain anatomy). Further research is thus required to establish the functional relevance of our findings. Last, while surface-based mapping allows for morphometric inferences on a sub-millimeter scale, the derived grey–white matter tissue intensity values, and hence the GWC, remain dependent on the native spatial resolution of the T1-weighted images (i.e., 1 mm isotropic). Thus, partial volume effects and/or the ability to clearly delineate the grey–white matter boundary may affect GWC values. However, both of these factors are expected to affect both groups equally, and our findings of significant between-group differences in GWC cannot be fully explained by these limitations.

Taken together, our findings suggest that DS is accompanied by a reduced tissue contrast between cortical grey and white matter and those differences in GWC seem to be able to explain some, albeit not all, of the differences in CT, which have previously been reported in DS. In addition, our study is the first to expand these previous reports to older adulthood, suggesting that the typical pattern of CT differences in DS remains stable across the lifespan.

CONFLICTS OF INTEREST

None of the authors have declared any conflict of interest or financial interests, which may arise from being named as an author on the manuscript.

ORCID

Anke Bletsch http://orcid.org/0000-0002-6857-4065

REFERENCES

Abanto, J., Ciamponi, A. L., Francischini, E., Murakami, C., de Rezende, N. P. M., & Gallottini, M. (2011). Medical problems and oral care of patients with Down syndrome: A literature review. *Special Care in Dentistry*, 31(6), 197–203. https://doi.org/10.1111/j.1754-4505.2011.00211.x

Ábrahám, H., Vincze, A., Veszprémi, B., Kravják, A., Gömöri, É., Kovács, G. G., & Seress, L. (2012). Impaired myelination of the human hippocampal formation in Down syndrome. *International Journal of Developmental Neuroscience*, 30(2), 147–158. https://doi.org/10.1016/j.ijdevneu.2011.11.005

Backhausen, L. L., Herting, M. M., Buse, J., Roessner, V., Smolka, M. N., & Vetter, N. C. (2016). Quality control of structural MRI images applied using FreeSurfer – A hands-on workflow to rate motion artifacts. *Frontiers in Neuroscience*, 10, https://doi.org/10.3389/fnins.2016.00558

Becker, L., Mito, T., Takashima, S., & Onodera, K. (1991). Growth and development of the brain in Down syndrome. *Progress in Clinical and Biological Research*, 373, 133–152.

Benavides-Piccione, R., Ballesteros-Yáñez, I., Martínez de Lagrán, M., Elston, G., Estivill, X., Fillat, C., ... Dierssen, M. (2004). On dendrites in Down syndrome and DS murine models: A spiny way to learn. *Progress in Neurobiology*, 74(2), 111–126. https://doi.org/10.1016/j.pneurobio.2004.08.001

Chakrabarti, L., Galdzicki, Z., & Haydar, T. F. (2007). Defects in embryonic neurogenesis and initial synapse formation in the forebrain of the Ts65Dn mouse model of Down syndrome. *Journal of Neuroscience*, 27(43), 11483–11495. https://doi.org/10.1523/JNEUROSCI.3406-07.2007

Dale, A. M., Fischl, B., & Sereno, M. I. (1999). Cortical surface-based analysis. *NeuroImage*, 9(2), 179–194. https://doi.org/10.1006/nimg.1998.0395

Dambska, M., & Laure-Kamionowska, M. (1990). Myelination as a parameter of normal and retarded brain maturation. *Brain & Development*, 12(2), 214–220. https://doi.org/10.1016/S0387-7604(12)80328-7

Davatzikos, C., & Resnick, S. M. (2002). Degenerative age changes in white matter connectivity visualized in vivo using magnetic resonance imaging. *Cerebral Cortex*, 12(7), 767–771. https://doi.org/10.1093/cercor/12.7.767

Dunn, L., Dunn, L., Whetton, C., & Burley, J. (1997). *The British Picture Vocabulary Scale* (2nd ed.). London, England: NFER Nelson.

Fischl, B., & Dale, A. M. (2000). Measuring the thickness of the human cerebral cortex from magnetic resonance images. *Proceedings of the National Academy of Sciences*, 97(20), 11050–11055. https://doi.org/10.1073/pnas.200033797

Fischl, B., Sereno, M. I., & Dale, A. M. (1999). Cortical surface-based analysis. *NeuroImage*, 9(2), 195–207. https://doi.org/10.1006/nimg.1998.0396

Geschwind, D. H., & Rakic, P. (2013). Cortical evolution: Judge the brain by its cover. *Neuron*, 80(3), 633–647. https://doi.org/10.1016/j.neuron.2013.10.045

Giedd, J. N., Blumenthal, J., Jeffries, N. O., Castellanos, F. X., Liu, H., Zijdenbos, A., ... Rapoport, J. L. (1999). Brain development during childhood and adolescence: A longitudinal MRI study. *Nature Neuroscience*, 2(10), 861–863. https://doi.org/10.1038/13158

Gogtay, N., Giedd, J. N., Lusk, L., Hayashi, K. M., Greenstein, D., Vaituzis, A. C., ... Thompson, P. M. (2004). Dynamic mapping of human cortical development during childhood through early adulthood. *Proceedings of the National Academy of Sciences*, 101(21), 8174–8179. https://doi.org/10.1073/pnas.0402680101

Golden, J. A., & Hyman, B. T. (1994). Development of the superior temporal neocortex is anomalous in trisomy 21. *Journal of Neuropathology & Experimental Neurology*, 53(5), 513–520. https://doi.org/10.1097/00005072-199409000-00011

Grydeland, H., Westlye, L. T., Walhovd, K. B., & Fjell, A. M. (2013). Improved prediction of Alzheimer's disease with longitudinal white matter/gray matter contrast changes. *Human Brain Mapping*, 34(11), 2775–2785. https://doi.org/10.1002/hbm.22103

Guidi, S., Bonasoni, P., Ceccarelli, C., Santini, D., Gualtieri, F., Ciani, E., & Bartesaghi, R. (2008). Neurogenesis impairment and increased cell death reduce total neuron number in the hippocampal region of fetuses with Down syndrome. *Brain Pathology*, 18(2), 180–197. https://doi.org/10.1111/j.1750-3639.2007.00113.x

Guidi, S., Ciani, E., Bonasoni, P., Santini, D., & Bartesaghi, R. (2011). Widespread proliferation impairment and hypocellularity in the cerebellum of fetuses with Down syndrome. *Brain Pathology*, 21(4), 361–373. https://doi.org/10.1111/j.1750-3639.2010.00459.x

Haier, R. J., Chueh, D., Touchette, P., Lott, I., Buchsbaum, M. S., MacMillan, D., ... Sosa, E. (1995). Brain size and cerebral glucose metabolic rate in nonspecific mental retardation and Down syndrome. *Intelligence*, 20(2), 191–210. https://doi.org/10.1016/0160-2896(95)90032-2

Haydar, T. F., Nowakowski, R. S., Yarowsky, P. J., & Krueger, B. K. (2000). Role of founder cell deficit and delayed neuronogenesis in microencephaly of the trisomy 16 mouse. *Journal of Neuroscience*, 20(11), 4156–4164. https://doi.org/10.1523/JNEUROSCI.20-11-04156.2000

Haydar, T. F., & Reeves, R. H. (2012). Trisomy 21 and early brain development. *Trends in Neurosciences*, 35(2), 81–91. https://doi.org/10.1016/j.tins.2011.11.001

Holtzman, D. M., Santucci, D., Kilbridge, J., Chua-Couzens, J., Fontana, D. J., Daniels, S. E., ... Mobley, W. C. (1996). Developmental abnormalities and age-related neurodegeneration in a mouse model of Down syndrome. *Proceedings of the National Academy of Sciences*, 93(23), 13333–13338. https://doi.org/10.1073/pnas.93.23.13333

Hon, J., Huppert, F. A., Holland, A. J., & Watson, P. (1999). Neuropsychological assessment of older adults with Down's Syndrome: An epidemiological study using the Cambridge Cognitive Examination (CAMCOG). *British Journal of Clinical Psychology*, 38(2), 155–165. https://doi.org/10.1348/014466599162719

Huppert, F. A., Brayne, C., Gill, C., Paykel, E. S., & Beardsall, L. (1995). CAMCOG-A concise neuropsychological test to assist dementia diagnosis: Socio-demographic determinants in an elderly population sample. *British Journal of Clinical Psychology*, 34(4), 529–541. https://doi.org/10.1111/j.2044-8260.1995.tb01487.x

Huttenlocher, P. R. (1984). Synapse elimination and plasticity in developing human cerebral cortex. *American Journal of Mental Deficiency*, 88(5), 488–496.

Huttenlocher, P. R. (1990). Morphometric study of human cerebral cortex development. *Neuropsychologia*, 28(6), 517–527. https://doi.org/10.1016/0028-3932(90)90031-I

Huttenlocher, P. R., & Dabholkar, A. S. (1997). Regional differences in synaptogenesis in human cerebral cortex. *Journal of Comparative Neurology*, 387(2), 167–178. https://doi.org/10.1002/(SICI)1096-9861(19971020)387:2<167::AID-CNE1>3.0.CO;2-Z

Jefferson, A. L., Gifford, K. A., Damon, S., Chapman, G. W., Liu, D., Sparling, J., . . . Salat, D. (2015). Gray & white matter tissue contrast differentiates mild cognitive impairment converters from non-converters. *Brain Imaging and Behavior*, 9(2), 141–148. https://doi.org/10.1007/s11682-014-9291-2

Jovicich, J., Czanner, S., Greve, D., Haley, E., van der Kouwe, A., Gollub, R., . . . Dale, A. (2006). Reliability in multi-site structural MRI studies: Effects of gradient non-linearity correction on phantom and human data. *NeuroImage*, 30(2), 436–443. https://doi.org/10.1016/j.neuroimage.2005.09.046

Kates, W. R., Folley, B. S., Lanham, D. C., Capone, G. T., & Kaufmann, W. E. (2002). Cerebral growth in fragile X syndrome: Review and comparison with Down syndrome. *Microscopy Research and Technique*, 57(3), 159–167. https://doi.org/10.1002/jemt.10068

Lee, N. R., Adeyemi, E. I., Lin, A., Clasen, L. S., Lalonde, F. M., Condon, E., . . . Giedd, J. N. (2016). Dissociations in cortical morphometry in youth with Down syndrome: Evidence for reduced surface area but increased thickness. *Cerebral Cortex*, 26(7), 2982–2990. https://doi.org/10.1093/cercor/bhv107

Lott, I. T., & Head, E. (2001). Down syndrome and Alzheimer's disease: A link between development and aging. *Mental Retardation and Developmental Disabilities Research Reviews*, 7(3), 172–178. https://doi.org/10.1002/mrdd.1025

Meguid, N. A., Fahim, C., Sami, R., Nashaat, N. H., Yoon, U., Anwar, M., . . . Evans, A. C. (2012). Cognition and lobar morphology in full mutation boys with fragile X syndrome. *Brain and Cognition*, 78(1), 74–84. https://doi.org/10.1016/j.bandc.2011.09.005

Mrak, R. E., & Griffin, W. S. T. (2004). Trisomy 21 and the Brain. *Journal of Neuropathology & Experimental Neurology*, 63(7), 679–685. https://doi.org/10.1093/jnen/63.7.679

Olmos-Serrano, JLuis., Kang, H. YO J. UNG., Tyler, W. ILLIAM A., Silbereis, J. OHN C., Cheng, F. ENG., Zhu, Y. ING., . . . Sestan, N. ENAD. (2016). Down syndrome developmental brain transcriptome reveals defective oligodendrocyte differentiation and myelination. *Neuron*, 89(6), 1208–1222. https://doi.org/10.1016/j.neuron.2016.01.042

Pardoe, H. R., Kucharsky Hiess, R., & Kuzniecky, R. (2016). Motion and morphometry in clinical and nonclinical populations. *NeuroImage*, 135, 177–185. https://doi.org/10.1016/j.neuroimage.2016.05.005

Pearlson, G. D., Breiter, S. N., Aylward, E. H., Warren, A. C., Grygorcewicz, M., Frangou, S., . . . Pulsifer, M. B. (1998). MRI brain changes in subjects with Down syndrome with and without dementia. *Developmental Medicine and Child Neurology*, 40(5), 326–334.

Pinter, J. D., Eliez, S., Schmitt, J. E., Capone, G. T., & Reiss, A. L. (2001). Neuroanatomy of Down's syndrome: A high-resolution MRI study. *American Journal of Psychiatry*, 158(10), 1659–1665. https://doi.org/10.1176/appi.ajp.158.10.1659

Rakic, P. (1988). Specification of cerebral cortical areas. *Science*, 241(4862), 170–176. https://doi.org/10.1126/science.3291116

Raznahan, A., Shaw, P., Lalonde, F., Stockman, M., Wallace, G. L., Greenstein, D., . . . Giedd, J. N. (2011). How does your cortex grow? *Journal of Neuroscience*, 31(19), 7174–7177. https://doi.org/10.1523/JNEUROSCI.0054-11.2011

Reuter, M., Tisdall, M. D., Qureshi, A., Buckner, R. L., van der Kouwe, A. J. W., & Fischl, B. (2015). Head motion during mri acquisition reduces gray matter volume and thickness estimates. *NeuroImage*, 107, 107–115. https://doi.org/10.1016/j.neuroimage.2014.12.006

Rueda, N., Flórez, J., & Martínez-Cué, C. (2013). Apoptosis in Down's syndrome: Lessons from studies of human and mouse models. *Apoptosis*, 18(2), 121–134. https://doi.org/10.1007/s10495-012-0785-3

Salat, D. H., Chen, J. J., van der Kouwe, A. J., Greve, D. N., Fischl, B., & Rosas, H. D. (2011). Hippocampal degeneration is associated with temporal and limbic gray matter/white matter tissue contrast in Alzheimer's disease. *NeuroImage*, 54(3), 1795–1802. https://doi.org/10.1016/j.neuroimage.2010.10.034

Salat, D. H., Lee, S. Y., van der Kouwe, A. J., Greve, D. N., Fischl, B., & Rosas, H. D. (2009). Age-associated alterations in cortical gray and white matter signal intensity and gray to white matter contrast. *NeuroImage*, 48(1), 21–28. https://doi.org/10.1016/j.neuroimage.2009.06.074

Schmidt-Sidor, B., Wisniewski, K. E., Shepard, T. H., & Sersen, E. A. (1990). Brain growth in Down syndrome subjects 15 to 22 weeks of gestational age and birth to 60 months. *Clinical Neuropathology*, 9(4), 181–190.

Ségonne, F., Dale, A. M., Busa, E., Glessner, M., Salat, D., Hahn, H. K., & Fischl, B. (2004). A hybrid approach to the skull stripping problem in MRI. *NeuroImage*, 22(3), 1060–1075. https://doi.org/10.1016/j.neuroimage.2004.03.032

Shaw, P., Kabani, N. J., Lerch, J. P., Eckstrand, K., Lenroot, R., Gogtay, N., . . . Wise, S. P. (2008). Neurodevelopmental trajectories of the human cerebral cortex. *Journal of Neuroscience*, 28(14), 3586–3594. https://doi.org/10.1523/JNEUROSCI.5309-07.2008

Sylvester, P. E. (1983). The hippocampus in Down's syndrome. *Journal of Intellectual Disability Research*, 27(3), 227–236. https://doi.org/10.1111/j.1365-2788.1983.tb00294.x

Vandekar, S. N., Shinohara, R. T., Raznahan, A., Roalf, D. R., Ross, M., DeLeo, N., . . . Satterthwaite, T. D. (2015). Topologically dissociable patterns of development of the human cerebral cortex. *Journal of Neuroscience*, 35(2), 599–609. https://doi.org/10.1523/JNEUROSCI.3628-14.2015

Vidal-Piñeiro, D., Walhovd, K. B., Storsve, A. B., Grydeland, H., Rohani, D. A., & Fjell, A. M. (2016). Accelerated longitudinal gray/white matter contrast decline in aging in lightly myelinated cortical regions. *Human Brain Mapping*, 37(10), 3669–3684. https://doi.org/10.1002/hbm.23267

Weijerman, M. E., & de Winter, J. P. (2010). Clinical practice: The care of children with Down syndrome. *European Journal of Pediatrics*, 169(12), 1445–1452.

Westlye, L. T., Walhovd, K. B., Dale, A. M., Espeseth, T., Reinvang, I., Raz, N., . . . Fjell, A. M. (2009). Increased sensitivity to effects of normal aging and Alzheimer's disease on cortical thickness by adjustment for local variability in gray/white contrast: A multi-sample MRI study. *NeuroImage*, 47(4), 1545–1557. https://doi.org/10.1016/j.neuroimage.2009.05.084

WHO (1992). Clinical descriptions and diagnostic guidelines. In WHO (Ed.), *The ICD-10 classification of mental and behavioural disorders*. Geneva, Switzerland: World Health Organization.

Wierenga, L. M., Langen, M., Oranje, B., & Durston, S. (2014). Unique developmental trajectories of cortical thickness and surface area. *NeuroImage*, 87, 120–126. https://doi.org/10.1016/j.neuroimage.2013.11.010

Wisniewski, K. E., & Schmidt-Sidor, B. (1989). Postnatal delay of myelin formation in brains from Down syndrome infants and children. *Clinical Neuropathology*, 8(2), 55–62.

Wisniewski, K. E., Wisniewski, H. M., & Wen, G. Y. (1985). Occurrence of neuropathological changes and dementia of Alzheimer's disease in Down's syndrome. *Annals of Neurology*, 17(3), 278–282. https://doi.org/10.1002/ana.410170310

Worsley, K. J., Andermann, M., Koulis, T., MacDonald, D., & Evans, A. C. (1999). Detecting changes in non-isotropic images. *Human Brain Mapping*, 8(2–3), 98–101. https://doi.org/10.1002/(SICI)1097-0193(1999)8:2/3<98::AID-HBM5>3.0.CO;2-F

Zhang, Y., Wu, Y., Zhu, M., Wang, C., Wang, J., Zhang, Y., . . . Jiang, T. (2011). Reduced cortical thickness in mental retardation. *PLoS One, 6* (12), e29673. https://doi.org/10.1371/journal.pone.0029673

SUPPORTING INFORMATION

Additional Supporting Information may be found online in the supporting information tab for this article.